Enzyme replacement prevents neonatal death, liver damage, and osteoporosis in murine homocystinuria

Tomas Majtan,*,[1] Helena Hůlková,[†,‡] Insun Park,* Jakub Krijt,[†] Viktor Kožich,[†] Erez M. Bublil,[§] and Jan P. Kraus*,[2]

*Department of Pediatrics, University of Colorado School of Medicine, Aurora, Colorado, USA; [†]Institute of Inherited Metabolic Disorders and [‡]Institute of Pathology, Charles University–First Faculty of Medicine and General University Hospital, Prague, Czech Republic; and [§]Orphan Technologies Limited, Rapperswil, Switzerland

ABSTRACT: Classical homocystinuria (HCU) is an inborn error of sulfur amino acid metabolism caused by deficient activity of cystathionine β-synthase (CBS), resulting in an accumulation of homocysteine and a concomitant decrease of cystathionine and cysteine in blood and tissues. In mice, the complete lack of CBS is neonatally lethal. In this study, newborn CBS-knockout (KO) mice were treated with recombinant polyethyleneglycolylated human truncated CBS (PEG-CBS). Full survival of the treated KO mice, along with a positive impact on metabolite levels in plasma, liver, brain, and kidneys, was observed. The PEG-CBS treatment prevented an otherwise fatal liver disease characterized by steatosis, death of hepatocytes, and ultrastructural abnormalities of endoplasmic reticulum and mitochondria. Furthermore, treatment of the KO mice for 5 mo maintained the plasma metabolite balance and completely prevented osteoporosis and changes in body composition that characterize both the KO model and human patients. These findings argue that early treatment of patients with HCU with PEG-CBS may prevent clinical symptoms of the disease possibly without the need of dietary protein restriction.—Majtan, T., Hůlková, H., Park, I., Krijt, J., Kožich, V., Bublil, E. M., Kraus, J. P. Enzyme replacement prevents neonatal death, liver damage, and osteoporosis in murine homocystinuria. FASEB J. 31, 5495–5506 (2017). www.fasebj.org

KEY WORDS: cystathionine β-synthase · homocysteine · PEGylation · preclinical drug development · rare inherited disease

Classical homocystinuria (HCU: OMIM 236200) represents the most common inherited defect of sulfur amino acid metabolism (1). It is a rare disease with a variable global birth prevalence of 1:100,000 to 1:200,000 (2). The underlying cause of HCU is a deficiency in enzyme activity of cystathionine β-synthase (CBS: EC 4.2.1.22). CBS is a heme-containing, S-adenosylmethionine (SAM)-activated, pyridoxal-5′-phosphate–dependent tetrameric enzyme catalyzing the condensation of serine and

homocysteine (Hcy) to form cystathionine (Cth) [reviewed by Majtan et al. (3)]. Cth is subsequently metabolized to cysteine (Cys), α-ketobutyrate, and ammonia by the action of the second enzyme of the trans-sulfuration pathway, Cth γ-lyase. Thus, Hcy, as an intermediate of the methionine cycle, is irreversibly directed to Cys synthesis by CBS activity. Consequently, the lack of CBS activity in patients with HCU is characterized by severely increased plasma and tissue levels of Hcy, methionine (Met), and S-adenosylhomocysteine (SAH) and, conversely, by decreased levels of Cth and Cys.

The clinical manifestations of untreated HCU include a combination of connective tissue defects, thromboembolism, stroke, osteoporosis, and mental retardation. There is no causal treatment available, but patients with HCU are prescribed either vitamin B_6 (to stimulate residual CBS activity) and/or a combination of protein-restricted diet (to limit Met intake), betaine (to divert Hcy conversion back to Met), and Cys supplements (to compensate for its deficiency). Although patients with early-diagnosed HCU after dietary restriction and/or betaine therapy have a very good prognosis (4), compliance with the diet usually worsens in adolescence and is particularly poor in late-diagnosed patients, leading to a high risk of complications (4). Therefore, an alternative therapeutic option is needed

that would: *1*) address the core deficiency, *2*) alleviate the requirement for stringent dietary regime, *3*) improve the metabolic control, and *4*) prevent the onset and/or progression of the clinical symptoms.

In 2016, we presented an enzyme replacement therapy (ERT) for HCU based on nonmodified dimeric human truncated CBS (htCBS) (5). When administered to an animal model of HCU, the enzyme showed very fast clearance from circulation and had no impact on plasma Hcy levels. This was overcome by conjugation of the enzyme to polyethylene glycol (PEG) moieties (5). In addition, introduction of the point mutation C15S into htCBS improved the solubility of the enzyme and enhanced reproducibility of the PEGylation using maleimide (MA) PEGs. The recombinant PEGylated htCBS C15S (PEG-CBS) presented with a substantially increased half-life compared with unmodified htCBS, decreased the levels of Hcy in plasma and tissues, and normalized Cys concentration in plasma. The recovery of the metabolic profile was accompanied by improvement of histopathological liver symptoms and substantially improved survival of the neonatally lethal CBS-knockout (KO) mice (5, 6). We then further improved PEG-CBS by testing and characterizing multiple conjugates of htCBS C15S with either MA- or *N*-hydroxysuccinimide (NHS) ester–activated PEG of different sizes and structures (7). The favored candidate for development was htCBS modified with 40-kDa linear MA PEG (40MA PEG-CBS), which formed distinct separable species with 1 or 2 PEGs attached to the C272 residue of the htCBS C15S dimer. However, PEGylation reproducibility and insufficient coverage of the enzyme most likely caused loss of efficacy after multiple rounds of injections followed by washout periods in homocystinuric mice (7). In contrast, PEGylation with a 20-kDa linear NHS ester PEG yielded a conjugate (20NHS PEG-CBS) that showed a sustained pharmacodynamic profile. In addition, the 20NHS PEG-CBS formed a homogeneous mixture of inseparable, highly PEGylated species with an estimated average PEGylation of 5.0 ± 0.5 PEGs per htCBS C15S monomer (7).

We assessed the efficacy of ERT for the most severely affected mouse HCU model, the CBS-KO mouse, experiencing neonatal lethality (6, 8). In addition to seeking comparison of potency of the leading candidates for the drug development (40MA or 20NHS PEG-CBS), we treated KO mice with either conjugate shortly after birth to determine whether such intervention would prevent early death and extend the lifespan of the KO mice. We correlated the results from the survival study with the plasma and tissue metabolites, liver histologic analyses, and changes in bone mineralization and body composition. We demonstrated that PEG-CBS in circulation serves as a metabolic sink, which improves or restores the plasma and tissue metabolic balance in the face of an unrestricted diet, resulting in the rescue of multiple pathologies associated with HCU.

MATERIALS AND METHODS

Chemicals

Unless stated otherwise, all materials were purchased from Sigma-Aldrich (St. Louis, MO, USA) or Thermo Fisher Scientific (Waltham, MA, USA). L-[U-^{14}C]-serine was obtained from PerkinElmer Life Sciences (Hopkinton, MA, USA).

Animals

All animal procedures were approved under animal protocol B-49414(03)1E by the University of Colorado Denver Institutional Animal Care and Use Committee, which is an Association of Assessment and Accreditation of Laboratory Animal Care-accredited (00235), Public Health Service–assured (A 3269-01), and U.S. Department of Agriculture-licensed (84-R-0059) institution. The CBS-KO mice (6) were purchased from The Jackson Laboratory (Bar Harbor, ME, USA) and propagated and genotyped as previously described (5). Animals were maintained on extruded standard diet 2918 (Envigo; Madison, WI, USA). A single-use lancet for submandibular bleeding was used for blood collection into Capiject T-MLHG lithium heparin (12.5 IU) tubes with gel (Terumo Medical, Elkton, MD, USA). Tubes were then centrifuged at 1200 g for 10 min, followed by transfer of plasma to 1.5-ml tubes and storage at $-80°C$.

Protein purification and PEGylation

htCBS C15S was expressed and purified as described in Bublil *et al.* (5). Purified enzyme was formulated and concentrated using the Labscale TFF system (EMD Millipore, Billerica, MA, USA) equipped with a Pellicon XL 50 Ultracel 30 cartridge (regenerated cellulose 30-kDa MWCO membrane) into 200 mM potassium phosphate (pH 6.5) or 100 mM sodium phosphate (pH 7.2). Activated PEG molecules with either an MA or NHS ester coupling group were purchased from NOF (Tokyo, Japan). PEGylation of htCBS with MA or NHS ester PEG was carried out in 100 mM potassium phosphate (pH 6.5) and 50 mM sodium phosphate (pH 7.2), respectively, by adding PEG dissolved in milliQ water (EMD Millipore) in the desired molar ratio (typically CBS subunit:PEG = 1:10) to a final protein concentration of 5 mg/ml. The reaction was carried out at 4°C overnight. Subsequently, the reaction mixture was diluted twice with milliQ water and buffer exchanged into Gibco 1× PBS (Thermo Fisher Scientific) and concentrated using a Labscale TFF system with Pellicon XL 50 Biomax 100 cartridge (polyethersulfone 100-kDa MWCO membrane).

Determination of metabolite concentrations

Plasma metabolites were determined by stable isotope dilution GC/MS as previously described (9). The analysis was performed in a blinded fashion without knowledge of the animal genotype and/or treatment regimen. Metabolites in liver, kidney, and brain homogenates and corresponding plasmas were determined using HPLC and LC-MS/MS as described elsewhere (8, 10, 11).

Histopathology

Mice euthanized using CO_2 followed by a cervical dislocation were perfused *via* an intracardiac catheter with 4% paraformaldehyde (PFA) in PBS (pH 7.4; Affymetrix, Santa Clara, CA, USA). Livers were dissected and divided into 2 portions: two thirds were used for light microscopy immersed in 4% PFA, and one third was cut into about 1-mm-thick slices and immersed into 3% glutaraldehyde (Electrom Microscopy Sciences, Hatfield, PA, USA) for electron microscopy. Tissues were kept in fixatives for at least 24 h at 4°C. Tissue blocks for histology were trimmed and dehydrated with a series of steps (ethanol, acetone, acetone-xylene mixture, and xylene)

and then embedded in paraffin. In parallel, small tissue blocks (around 4 × 2 mm) fixed with paraformaldehyde were rapidly frozen in petrol ether cooled with dry ice and stored at −50°C for detection of apolar lipids. Fixed tissue was sectioned (4-μm-thick slices), placed on slides, and deparaffinized in xylene and isopropanol followed by rehydration with a series of graded ethanol/water baths (96, 70, and 60%). Tissue sections were stained with hematoxylin and eosin for histopathology. Masson trichrome staining was performed for detection of fibrosis. Steatosis was verified using Oil Red O staining for detection of apolar lipids in fixed frozen sections (10 μm thick) and cut with a Leica CM 1850 Cryomicrotome (Leica Microsystems, Wetzlar, Germany). The sections were viewed and photographed in a Nikon E800 light microscope (Nikon, Tokyo, Japan) equipped with an Olympus DP70 digital camera (Olympus, Tokyo, Japan). Samples fixed in 3% glutaraldehyde were subsequently postfixed with 1% osmium tetraoxide, dehydrated with an ethanol series and propylene oxide, and embedded into a Durcupan-Epon mixture. Ultrathin sections were double contrasted with uranyl acetate and lead nitrate and examined using a Jeol 1200 transmission electron microscope (Jeol Ltd., Akishima, Japan). The pathologist was blinded to the treatment regimen of the individual mice, and untreated, aged-matched WT mice served as a comparator.

Dual-energy X-ray absorptiometry measurement

Osteoporosis and body composition were assessed in anesthetized mice (60 mg/kg ketamine and 15 mg/kg xylazine in PBS injected, i.p.) using a GE Lunar PIXImus scanner (Lunar, Madison, WI, USA). Mice were placed on a tray with their abdomen down and scanned from the neck down excluding the tail. After the scan, the mice were returned to their cage to recover.

Statistical analysis

All data are presented as means ± SEM. Statistical comparisons of 2 groups were conducted using an unpaired, 2-tailed Students t test. Statistical analysis of 3 or more factor levels was conducted by ANOVA followed by Tukey's multiple comparison test to determine significance. A log-rank test was used for comparison of the 2 individual survival curves, and significance was calculated using the χ^2 test.

RESULTS

PEG-CBS prevents neonatal lethality and extends lifespan of CBS-KO mice

Two PEG-CBS candidates (40MA and 20NHS PEG-CBS) (7) were administered to CBS-KO mice from d 2 after birth. The mice were treated 3 times a week with a dose of 7.5 mg/kg administered subcutaneously. The dose of 7.5 mg/kg was selected based on a single-injection pharmacokinetics-pharmacodynamics studies performed in a nonlethal murine model of HCU, which showed that maximal efficacy response could be achieved by dosing 5–10 mg/kg (data not shown). The dose was adjusted to the average weight of the pups on each day during the neonatal period (prior to weaning on d 21) and then to the individual weight of the weaned mice (d 21 and on). Only 20% of the PBS-injected KO mice (n = 44) survived to weaning, with median survival of 17 d, compared with 96% survival in mice treated with 40MA (n = 18 M + 13 F) or 20NHS PEG-CBS (n = 14 M + 14 F) (**Fig. 1A**). None of the PBS-injected animals survived beyond d 29, whereas at least 93% of the PEG-CBS–treated KO mice were alive on d 35 (median survival could not be determined because more than 50% of mice survived the full term of the study).

Because mice survived beyond d 35, we continued to monitor the effect of the treatment on lifespan extension (Fig. 1B). Selected mice that survived up to d 35 and had
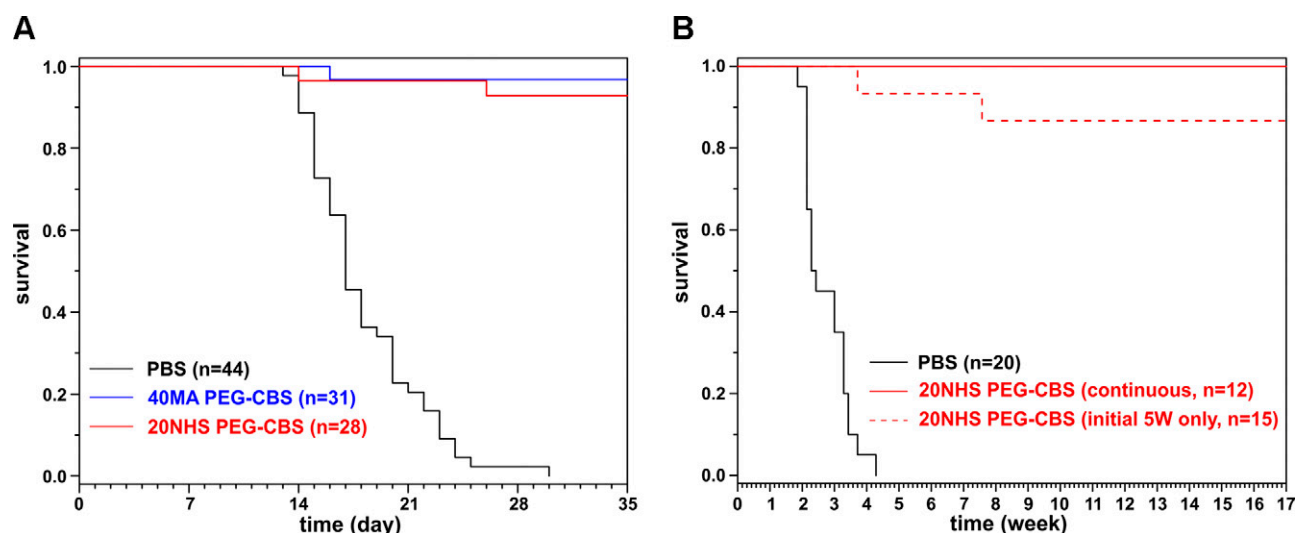
Figure 1. Rescue of KO mouse neonatal lethality by PEG-CBS administration. *A*) Kaplan-Meier survival curves of KO mice that were injected subcutaneously 3 times weekly with 7.5 mg/kg of 40MA (blue) or 20NHS (red) PEG-CBS *vs.* similarly treated PBS-injected KO mice (black). Mice were maintained on betaine water until weaning (d 21). *P* < 0.00001, PBS *vs.* 40MA/20NHS PEG-CBS–injected mice; *P* = 0.49, 40MA *vs.* 20NHS. *B*) Kaplan-Meier survival curves of surviving KO mice followed beyond the initial 5-wk treatment up to 17 wk of age. The KO mice, which received 20NHS PEG-CBS during the first 5 wk and survived, were divided into 2 groups: the first cohort continued with the similar treatment up to 17 wk of age (continuous, solid red line); the second cohort was left untreated beyond the initial 5-wk treatment (initial 5 wk only, dashed red line). PBS-injected KO mice (black solid line) are shown for comparative purposes. *P* < 0.00001, PBS *vs.* 20NHS (CONT/5 W); *P* = 0.19, 20NHS CONT *vs.* 20NHS 5W.

been treated with 20NHS PEG-CBS were divided into 2 groups. The first group received no further treatment except for the initial 5 wk of dosing. The second group continued with 3 times a week of 20NHS PEG-CBS subcutaneous injections (7.5 mg/kg). Mice in both groups survived up to 4 mo of age, at which stage the experiment was terminated. There was not a single death recorded among the continuously treated mice during this period, whereas a survival rate of 86% was recorded for the group that received treatment only during the initial 5 wk. Although most of the mice were euthanized for the terminal endpoint studies, those that were spared readily survived beyond a year of age (data not shown).

Partial normalization of metabolic control is sufficient to drive an almost complete rescue of the neonatal lethality in treated animals

During the survival study (initial 35 d), no plasma samples were taken because bleeding may lead to the death of the animal. To verify that the injected enzyme is catalytically competent once it enters the bloodstream from the subcutaneous injection site, the surviving mice ($n = 15$ M + 10 F and 16 M + 11 F for the 40MA and 20NHS PEG-CBS–treated mice, respectively) were first bled after a weekend washout (Monday; 3 d after the last injection) at the end of 5-wk PEG-CBS dosing (trough), then injected again and bled 24 h later (peak) and compared with a healthy PBS-injected heterozygous sibling ($n = 14$ M + 13 F). A weekend washout resulted in accumulation of plasma Hcy and concurrent depletion of Cys levels, which were substantially improved by an additional dose of PEG-CBS but were not normalized to the levels determined in heterozygous mice (**Fig. 2A**). Plasma methionine was slightly elevated compared with the controls and was not substantially affected by the PEG-CBS treatment. Plasma Cth levels remained similar at trough and peak of CBS activity, suggesting slow renal clearance, continuous production by a residual PEG-CBS, and/or saturation of blood distribution capacity. Both forms of PEG-CBS (40MA and 20NHS) performed similarly well; however, 20NHS PEG-CBS had a more pronounced effect on the correction of plasma Hcy and Cys levels than 40MA PEG-CBS (Fig. 2A).

Weight often serves as an easily accessible marker of overall health and well-being of the animals. Thus, body weights and weight gains of 20NHS PEG-CBS–treated mice were determined every other day from weaning (d 21) up to 35 d of age and compared with sex- and age-matched PBS-treated heterozygous control mice (Fig. 2B, C, respectively). At the time of weaning (d 21), no significant differences were found in body weights of the studied mice except for a slightly higher weight of the 20NHS PEG-CBS–treated KO male mice ($P < 0.01$). From d 25 on, the male control mice exhibited significant increases in weight compared with the remaining groups ($P < 0.001$) (Fig. 2B). The KO mice temporarily experienced a slower growth right after weaning (d 21–25) compared with the control mice (Fig. 2B, C). Interestingly, the treated KO male and female mice gained weight similarly quickly

but overall more slowly than the control mice. Our results show that administration of 20NHS PEG-CBS allowed for slower but steady growth of treated KO mice compared with the PBS-injected healthy control mice.

PEG-CBS in circulation results in improved or normalized tissue sulfur amino acid metabolites

Our initial data on the less-severe HCU mouse model (HO, human only) suggested that the PEG-CBS in circulation may serve as a metabolic sink that constantly and systematically removes Hcy from the plasma, resulting in improved metabolic balance in tissues (5). We tested this hypothesis with the most severe HCU mouse model, KO. Because most untreated KO mice do not survive, we determined metabolites in plasma and selected tissues (liver, kidney, and brain) in 18-d-old untreated KO mice and compared them with age-matched untreated healthy WT mice and 20NHS PEG-CBS–injected KO mice (from d 2 of age; 3 times a week, 7.5 mg/kg). **Figure 3** and Supplemental Table 1 show that the infant KO mice showed a substantial sulfur amino acid metabolic imbalance compared with healthy WT mice in circulation and in the tissues. Hcy was greatly increased in plasma and tissues compared with WT control mice (on average 26 times more in plasma and 6-fold higher in tissues compared with WT mice) (Fig. 3A). On the other hand, downstream products of the transsulfuration pathway were significantly reduced (Cys; Fig. 3B) or almost undetected (Cth; Fig. 3C). Interestingly, although total Cys levels in plasma and non–protein-bound Cys in liver were reduced to ~40% of that in WT mice, the concentration of non–protein-bound Cys did not seem to be different in kidney and brain of KO mice compared with WT control mice (Fig. 3B). Levels of Cth in plasma and tissues of untreated KO mice were reduced to 2–7% of those determined in WT mice (Fig. 3C). In addition to Hcy, a lack of CBS activity in KO mice resulted in a substantial increase of Met, an upstream metabolite of the methionine cycle (Fig. 3D). Plasma and liver/kidney/brain Met concentrations were increased 5.5- and 13-/7.6-/10-fold compared with those found in WT mice. Administration of 20NHS PEG-CBS to KO mice resulted in a significant improvement or total normalization of the metabolites. Specifically, plasma and liver/kidney/brain levels of Hcy were significantly decreased by 80 and 65/90/95%, respectively, compared with untreated KO mice (Fig. 3A). Whereas Hcy levels in plasma of the 20NHS PEG-CBS–treated KO mice remained somewhat elevated compared with those in WT control mice, the Hcy concentrations in tissues of treated KO mice were normalized. Cys was significantly increased in the treated KO mice compared with untreated KO control mice in plasma and in liver (Fig. 3B). More importantly, levels of Cys in plasma and all tissues were normalized by the treatment in KO mice. CBS activity in circulation of the treated KO mice resulted in a massive accumulation of Cth in plasma and kidney compared with both the untreated KO mice
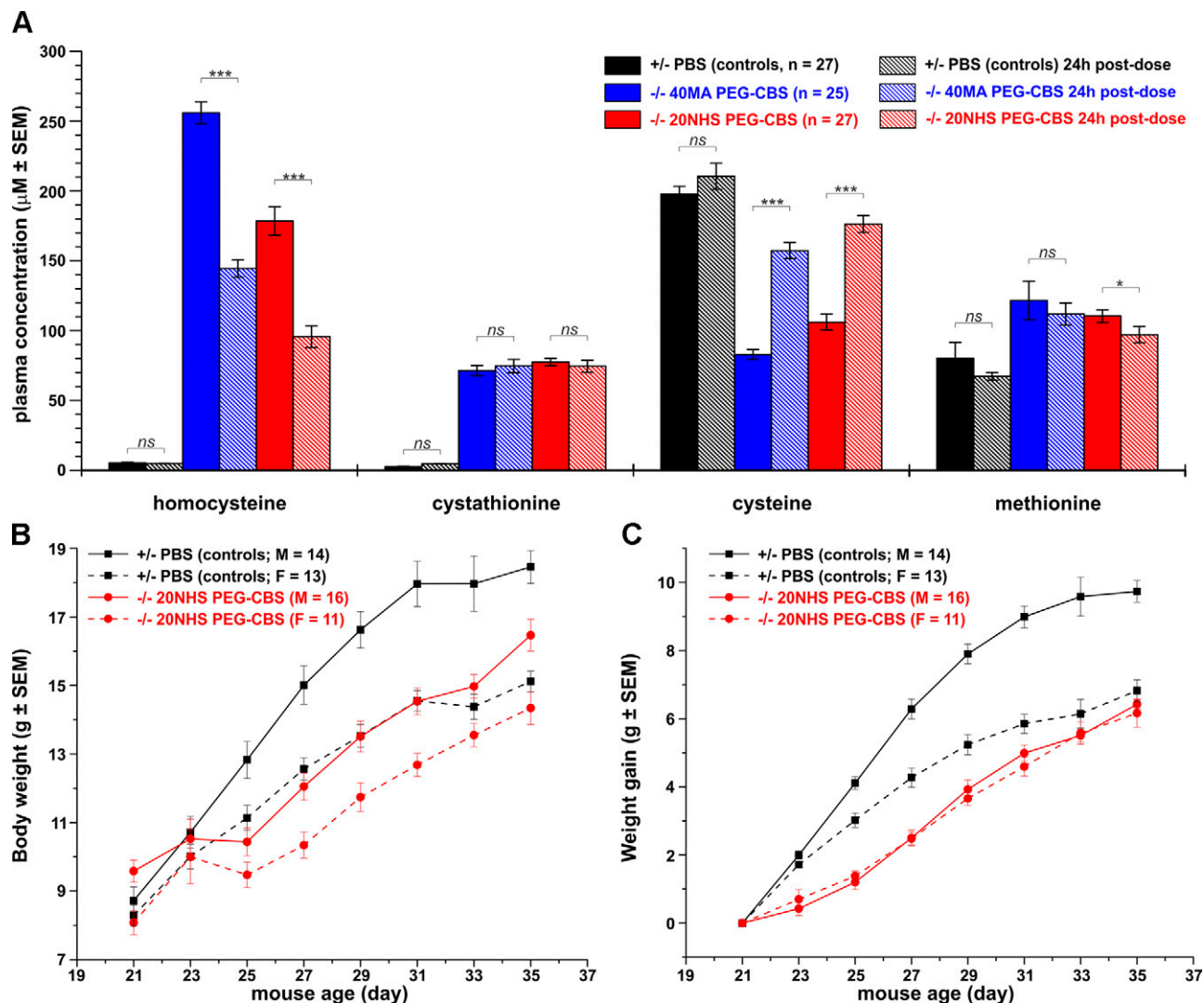
Figure 2. Plasma metabolites, body weight, and weight gain as markers of successful rescue of KO mice with PEG-CBS treatment. *A*) Plasma concentrations of Hcy, Cth, Cys, and Met after weekend washout (trough, solid bars) and 24 h after the last injection (peak, hatched bars) of 40MA (blue) or 20NHS (red) PEG-CBS compared with PBS-injected heterozygous siblings (black). *B, C*) Body weight (*B*) and weight gain (*C*) of 20NHS PEG-CBS–treated CBS-KO male (red solid line and circles) and female (red dashed line and circles) mice compared with PBS-injected heterozygous male (black solid line and squares) and female mice (black dashed line and squares). The number of subjects in each group is indicated in the plots. Mice received subcutaneous injections 3 times a week of 7.5 mg/kg from d 2 of age until d 35. *$P < 0.05$, ***$P < 0.001$.

and WT control mice (Fig. 3*C*). Cth in liver of the treated KO mice was normalized to WT levels but was only modestly increased in brain compared with WT animals, although it was significantly elevated compared with untreated KO mice. Finally, severe hypermethioninemia found in untreated KO mice was prevented with the treatment and Met levels in plasma, and tissues were normalized to those found in WT mice (Fig. 3*D*).

In addition to sulfur amino acids in plasma and tissues, Fig. 3 and Supplemental Table 1 show the levels of the main cellular redox molecule, reduced glutathione (GSH) (Fig. 3*E*), and the methylation index (SAM/SAH ratio, Fig. 3*F*; individual SAM and SAH levels are shown in Supplemental Table 1). The GSH concentration in plasma is very low (~30 μM) compared with the tissues (>1 μM/g of tissue), confirming the major role GSH plays inside the cell. The

levels of GSH were not found substantially different between healthy WT and homocystinuric KO mice or between 20NHS PEG-CBS–treated and untreated KO mice. A somewhat higher GSH level in the kidney homogenate from KO mice compared with the treated ones was the only significant difference found for this metabolite ($P < 0.05$). In contrast, the methylation index in plasma and tissues was substantially and significantly decreased in KO mice compared with WT control mice (Fig. 3*F*). Administration of 20NHS PEG-CBS significantly improved the SAM/SAH ratio in plasma and tissues of the treated KO mice compared with the untreated KO mice but did not normalize it to the levels seen in WT control mice. The SAM/SAH ratio was quite small in the livers of WT control mice compared with plasma and other tissue levels and, more importantly, was comparable to the
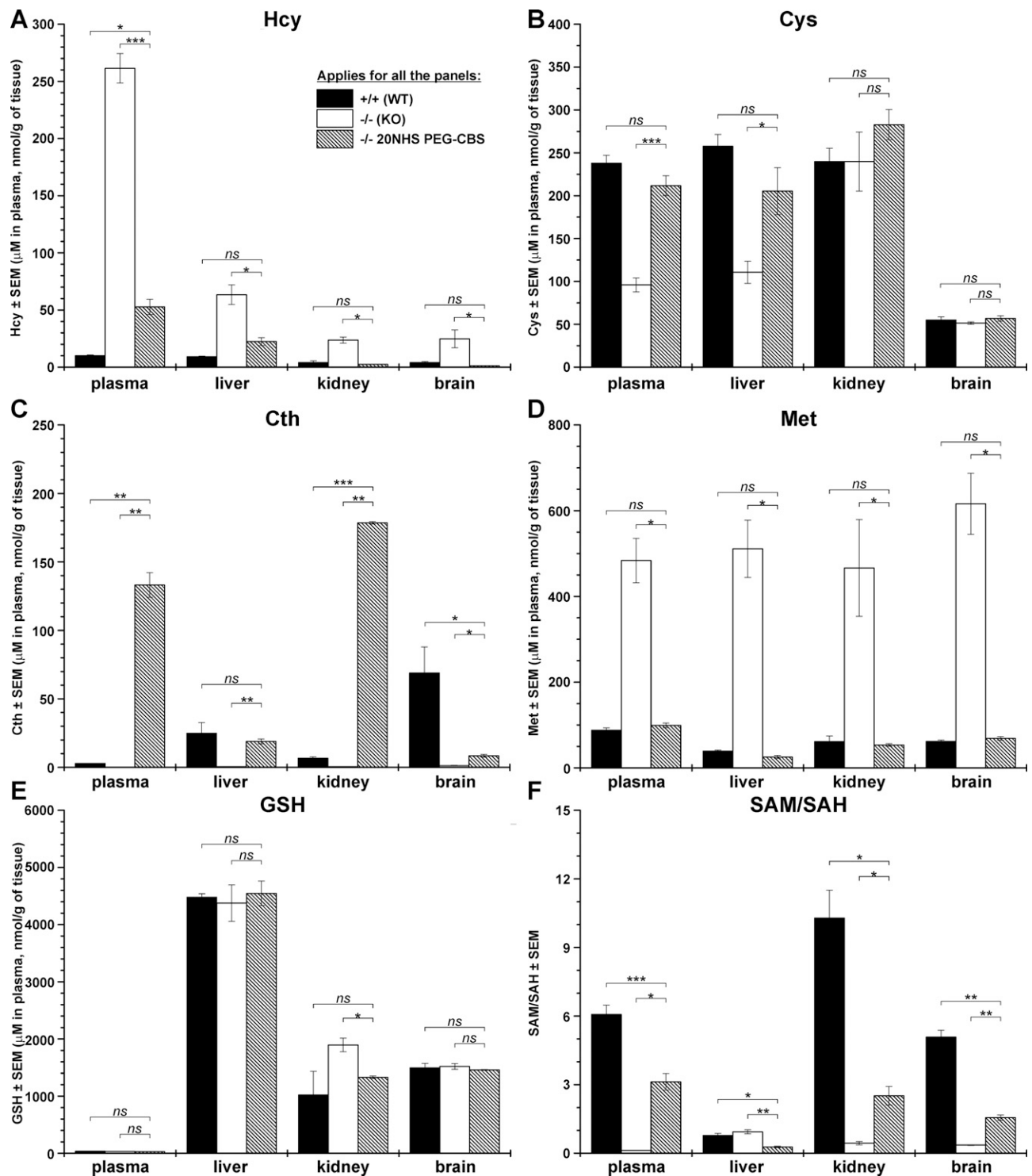
Figure 3. Plasma and tissue levels of sulfur metabolites in untreated or 20NHS PEG-CBS–injected KO mice compared with untreated WT mice. The following metabolites are displayed in individual panels: Hcy (*A*), Cys (*B*), Cth (*C*), Met (*D*), GSH (*E*), and the methylation index (SAM/SAH ratio) (*F*). Total Hcy and Cys were determined in plasma, whereas the non–protein-bound fraction of these thiols was measured in tissue homogenates. Treated KO mice were dosed 3 times a week (7.5 mg/kg) from d 2 of age. Each group consisted of 3–4 18-d-old mice. *$P < 0.05$, **$P < 0.01$, ***$P < 0.001$.

levels found in KO mice. In addition, the 20NHS PEG-CBS treatment further decreased the SAM/SAH ratio in the treated KO mice compared with untreated ones. Our results show that administration of 20NHS PEG-CBS improved or restored the metabolic balance in plasma and tissues of the treated KO mice.

PEG-CBS treatment prevents liver steatosis and necrosis of hepatocytes

It was shown previously that KO mice experience severe liver damage (8) and that administration of PEG-CBS prevented progression of these pathologic changes (5).

Improved KO mouse survival and metabolic balance in plasma and tissues suggested that the prevention of liver damage could be crucial for mouse survival. For that reason, liver histopathology was assessed to determine the effect of the treatment on livers of the KO mice. Because the mean survival half-life of PBS-injected KO mice was only 17 d, we analyzed, in a blinded fashion, livers from KO mice injected 3 times a week (SC, 7.5 mg/kg) with PBS ($n = 5$ M + 5 F), 40MA PEG-CBS ($n = 2$ M + 1 F), or 20NHS PEG-CBS ($n = 2$ M + 3 F) and euthanized on 18 ± 1 d of age. Age-matched livers from similarly treated healthy heterozygous ($n = 1$ M + 2 F) and untreated WT mice ($n = 1$ M + 1 F) served as unaffected controls. No significant differences in liver histology were found between the healthy control mice (untreated WT and heterozygous mice received either PBS or 20NHS PEG-CBS; data not shown).

Figure 4 illustrates the liver histopathology using light microscopy. Control mice (PBS-treated heterozygous animals) exhibited liver parenchyma with a regular architecture (Fig. 4*A*). A detailed look showed hepatocytes with normally sized and regularly shaped nuclei with fine chromatin, inconspicuous nucleoli, and occasionally detectable discrete lipid droplets in the cytoplasm (Fig. 4*B*). In contrast, the PBS-injected KO mice developed moderate to severe hepatopathy characterized by substantial steatosis of a mixed type and focal hepatocellular necroses with resorptive inflammatory reaction (Fig. 4*C*). In addition, pleiomorphic, enlarged hyperchromatic nuclei with prominent nucleoli were observed (Fig. 4*D*). Signs denoting regeneration of the liver parenchyma (mitoses, binucleated hepatocytes) were rare, and fibrosis was not detected in these samples. Treatment with either PEG-CBS conjugate resulted in a more regular architecture of the liver lobule, less pronounced nuclear changes in hepatocytes, and essentially no signs of the hepatocellular death or increased regeneration of the liver parenchyma (Fig. 4*E–H*). In general, treatment with the 20NHS PEG-CBS yielded somewhat better results than with 40MA PEG-CBS. In particular, 40MA PEG-CBS–treated KO mice showed slightly irregular architecture of liver parenchyma with mild microvesicular steatosis and some enlarged hyperchromatic nuclei with conspicuous nucleoli (Fig. 4*E, F*). Findings in liver from 20NHS PEG-CBS–treated KO mice showed minimal changes and an overall picture reminiscent of that found in healthy control mice (Fig. 4*G, H*).

Electron microscopy of parallel samples provided a much more detailed representation of cellular structures and essentially corroborated the findings observed by light microscopy (**Fig. 5**). Control animals (PBS-treated heterozygous mice) showed hepatocytes with regular nuclei and normal composition of the cytoplasm (Fig. 5*A*), with slim and normally organized rough endoplasmic reticulum (ER) cisternae, normally sized and shaped mitochondria with regular cristae, and a usual amount of cytosolic glycogen (Fig. 5*B*). In contrast, hepatocytes of PBS-injected KO mice exhibited atypical composition of cytoplasm with numerous vesicles and fragmented cisternae and an increased number of mitochondria. Accumulation of lipid droplets in the cytoplasm of hepatocytes and the presence of enlarged hyperchromatic nuclei with irregular outlines, chromatin clumping, and prominent nucleoli detected by light microscopy were confirmed (Fig. 5*C*). Higher magnification further revealed variably increased width of cisternae of ER and mitochondria swelling with disorganized cristae (Fig. 5*D*). Treatment with either PEG-CBS conjugate resulted in overall normal composition of the cytoplasm of hepatocytes, with slim and normally organized cisternae of rough ER and predominantly normal mitochondria with regular cristae (Fig. 5*E–H*). Cytoplasmic vesicles and cisternae were neither increased in number nor dilated. Again, the observed pathologic changes were less pronounced in livers from mice treated with 20NHS PEG-CBS than with 40MA PEG-CBS. In particular, hepatocytes of the 40MA PEG-CBS–treated KO mice showed more slightly enlarged mitochondria, occasional lipid droplets in the cytoplasm, and some hyperchromatic nuclei (Fig. 5*E, F*). Hepatocytes from the 20NHS PEG-CBS–treated KO mice showed overall normal composition of the cytoplasm and regular normochromatic nuclei, and, in general, they were indistinguishable from the control mice (Fig. 5*G, H*). Taken together, CBS deficiency in KO mice resulted in severe hepatopathy with profound steatosis, which was substantially ameliorated by enzyme replacement therapy.

Long-term PEG-CBS treatment prevents osteoporosis and changes in body composition

Survival of the KO mice administered 20NHS PEG-CBS allowed us to study the long-term efficacy of the ERT on clinically relevant endpoints, such as osteoporosis, a hallmark of HCU manifestation in humans. **Figure 6** shows plasma biochemical balance of the treated KO mice ($n = 5$ M + 7 F) sustained by a continuous 3 weekly 20NHS PEG-CBS injections (7.5 mg/kg SC). Note that the initial levels at d 42 do not represent the true basal concentrations of the metabolites prior to treatment initiation because the KO mice were treated from 2 d of age. Instead, the initial levels correspond to plasma concentration of the metabolites 72 h after the injection (*i.e.*, after a weekend washout), when mice were old enough to survive blood collection. Dosing with 20NHS PEG-CBS resulted in a significant improvement of plasma metabolites on d 45 compared with the initial levels, leading to a substantial decrease of Hcy (180.3 *vs.* 85.3 μM; $P < 0.001$), a modest drop in Cth (73.4 *vs.* 42.8 μM; $P < 0.001$), and normalization of Cys (96.0 *vs.* 185.6 μM; $P < 0.001$). Improved levels were sustained with a regular dosing up to ~5 mo of age, when the efficacy of the ERT on the clinically relevant endpoint was assessed by dual-energy X-ray absorptiometry (DXA).

Figure 7 compares bone mineralization and body composition of age-matched healthy untreated KO heterozygous mice ($n = 4$ M + 6 F) with affected KO mice ($n = 5$ M + 10 F) left untreated from d 35 and continuously treated KO mice ($n = 5$ M + 7 F). Compared with healthy control mice, the KO mice developed significant osteoporosis characterized by decreased bone mineral density (0.050 *vs.* 0.045 g/cm^2; $P < 0.001$) (Fig. 7*A*) and bone mineral content (0.429 *vs.* 0.354 g; $P < 0.05$) (Fig. 7*B*). On the other hand, continued treatment of KO mice with
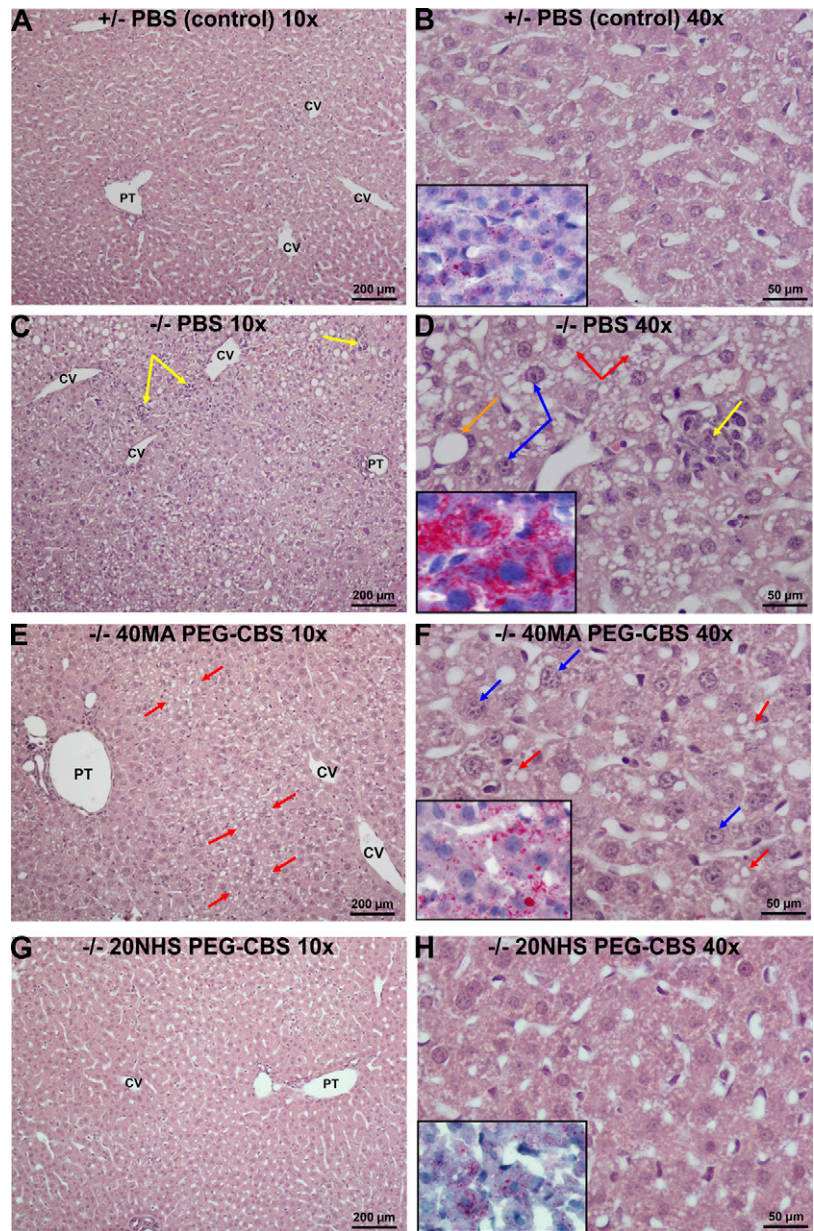
Figure 4. Effect of PEG-CBS treatment on liver histopathology of KO mice at the light microscopy level. PBS-injected healthy heterozygous mice (*A, B*) served as controls. Liver findings in PBS-injected KO mice (*C, D*) were compared with the ones from 40MA (*E, F*) and 20NHS (*G, H*) PEG-CBS–treated KO mice (SC, 3×/wk, 7.5 mg/kg). The left panels (*A, C, E, G*) show low-magnification views (original magnification, ×10; scale bars, 200 μm). The right panels (*B, D, F, H*) display higher magnification views (original magnification, ×40; scale bars, 50 μm) of hematoxylin and eosin–stained liver parenchyma. Insets in the right panels illustrate Oil Red O–specific stain for apolar lipids in the cytoplasm of hepatocytes. Yellow arrows point to focal hepatocellular necroses with resorptive inflammatory reaction. Orange and red arrows designate micro- and macro-vesicular steatosis, respectively. Blue arrows denote enlarged hyperchromatic nuclei and prominent nucleoli. CV, central vein; PT, portal tract.

20NHS PEG-CBS resulted in no signs of osteoporosis (bone mineral density, 0.053 g/cm^2; bone mineral content, 0.443 g) compared with healthy control mice [P = nonsignificant (ns)] and affected KO mice ($P < 0.001$). Total mass (20.28 *vs.* 24.00 g; $P < 0.05$) and fat content (12.74 *vs.* 19.90%; $P < 0.001$), but not the amount of lean mass (17.69 *vs.* 18.04 g; P = ns), of the KO mice was also significantly decreased compared with healthy heterozygous mice (Fig. 7*C*–*E*). Continuous treatment of KO mice significantly improved all 3 body composition parameters (total mass, 23.37 g; lean mass, 19.53 g; fat content, 15.97%) compared with affected KO mice ($P < 0.05$) and essentially normalized them compared with healthy control mice (P = ns). Interestingly, continuous treatment of KO mice with 20NHS PEG-CBS seemed to slightly increase the amount of lean mass at the expense of fat tissue compared with healthy control subjects, whereas total mass remained essentially identical. Continuous ERT administration from

birth prevented osteoporosis and negative changes in body composition in KO mice.

DISCUSSION

There have been no advances in the treatment of HCU since the introduction of the methionine-restricted diet and pyridoxine in 1960s and of betaine administration in 1980s (12–14). Treatment with pyridoxine is efficient in ~50% of patients, with some residual enzyme activity and a generally milder form of HCU. A low-protein diet and/or betaine prevents thromboembolism, lens dislocation, and cognitive impairment in patients detected early by newborn screening and adhering to the prescribed treatment (4). However, compliance of patients with late-diagnosed HCU with the low-Met diet and/or betaine is often poor (15). Thus, there is a need for an additional treatment
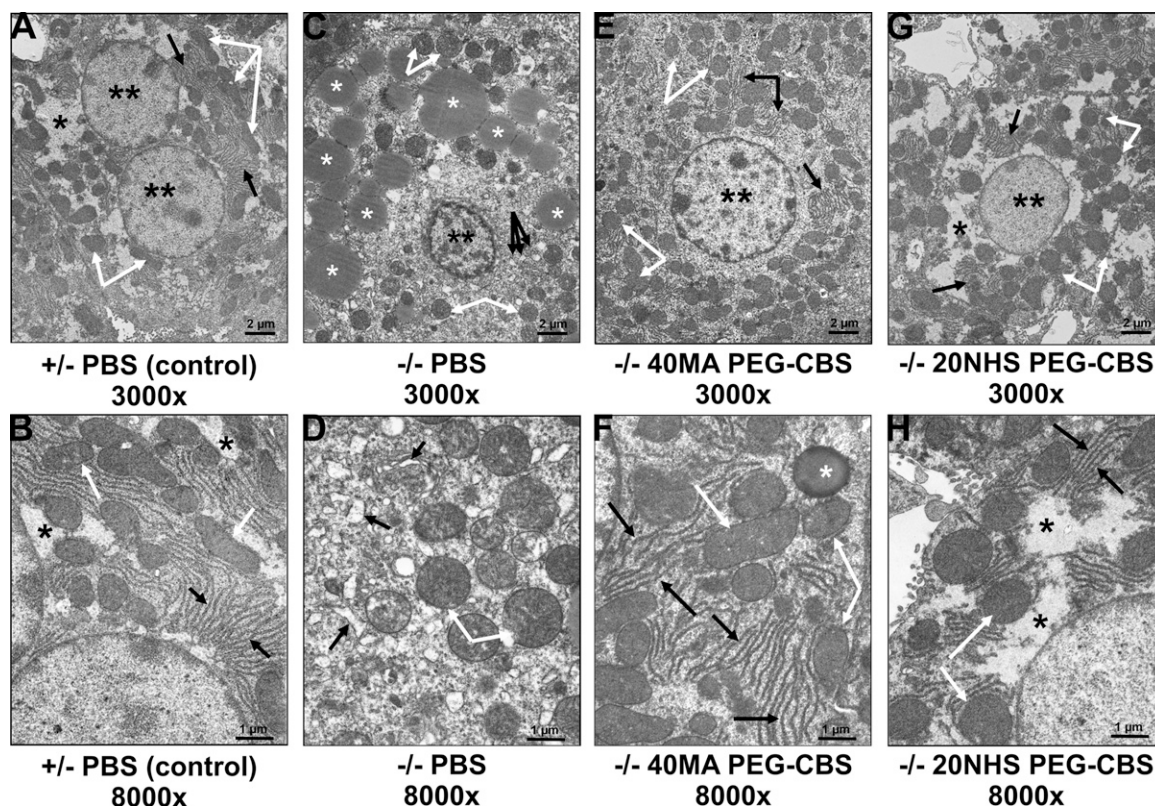
Figure 5. Effect of PEG-CBS treatment on liver histopathology of KO mice at the electron microscopic level. PBS-injected healthy heterozygous mice (*A, B*) served as controls. Ultrastructure of hepatocytes in PBS-injected KO mice (*C, D*) was compared with the ones from 40MA (*E, F*) and 20NHS (*G, H*) PEG-CBS–treated KO mice (SC, 3×/wk, 7.5 mg/kg). Top panels (*A, C, E, G*) show low-magnification views (original magnification, ×3000; scale bars, 2 μm). Bottom panels (*B, D, F, H*) display higher magnification views (original magnification, ×8000; scale bars, 1 μm). Double black asterisks designate nuclei; single black asterisks denote cytosolic glycogen. White asterisks indicate lipid droplets. White arrows point to mitochondria (swollen in *C* and *D*). Black arrows direct to rough endoplasmic reticulum in all panels except *C*, where black arrows designate numerous cytoplasmic cisternae and vesicles seen at lower magnification.

option that would achieve the desired therapeutic goals without the strict dietary requirements. As shown here, a novel ERT based on PEGylated human truncated CBS and its remarkable efficacy on the lethal form of murine HCU may represent such a treatment option.

The lack of CBS activity in KO mice results in a neonatally lethal phenotype (6). Neither supplementation of the depleted end product of the transsulfuration pathway, namely Cys, nor administration of betaine to decrease Hcy levels could increase the mean survival (8). On the other hand, our initial attempt with the ERT, using a different PEG-CBS molecule, resulted in an ~60% increase in median survival (to 27 d) of the treated mice compared with the PBS-injected KO mice (5). Even such a remarkable improvement in KO mice survival falls short in comparison with the latest conjugates shown here yielding >93% mice surviving after the initial 5 wk of treatment (Fig. 1*A*). More importantly, the majority of KO mice readily survived to 5 mo of age regardless of treatment continuation after the initial 5 wk (Fig. 1*B*). Plasma metabolites were not entirely normalized, but PEG-CBS administration led to a substantial decrease of Hcy and a concomitant increase of Cys in plasma of the surviving KO mice accompanied by a slower but steady growth (Fig. 2). Compared with the previously used dosing schedule (5), here we took extra care to maintain the right dose in infant mice and, more importantly, injected the mice 3 times a week rather than twice a week. The elimination half-life of various PEG-CBS in mice was calculated to range between 15 and 30 h (5), and thus 3 weekly injections most likely sustained a sufficient exposure and prevented spikes in metabolites compared with 2 weekly doses.

In addition to plasma metabolites, PEG-CBS activity in circulation yielded an improved or even entirely normalized metabolite profile in tissues (Fig. 3). This finding confirms the hypothesis that PEG-CBS does not necessarily need to be delivered into its native intracellular milieu. Instead, high availability of the substrate in circulation makes the blood an ideal target compartment, with an additional benefit of PEG-CBS functioning as a sink by forming a concentration gradient between tissues and plasma. Our previous data suggested that Hcy decreases significantly in tissues with PEG-CBS treatment in mice (5). We confirmed this initial observation and showed that, in addition, ERT normalized the Cys levels, increased Cth levels, and improved the SAM/SAH ratio in plasma and tissues. Interestingly, infant KO mice showed a severe elevation of Met levels, which were normalized in plasma and tissues with the treatment. The mild improvement but no normalization of SAM/SAH ratio in
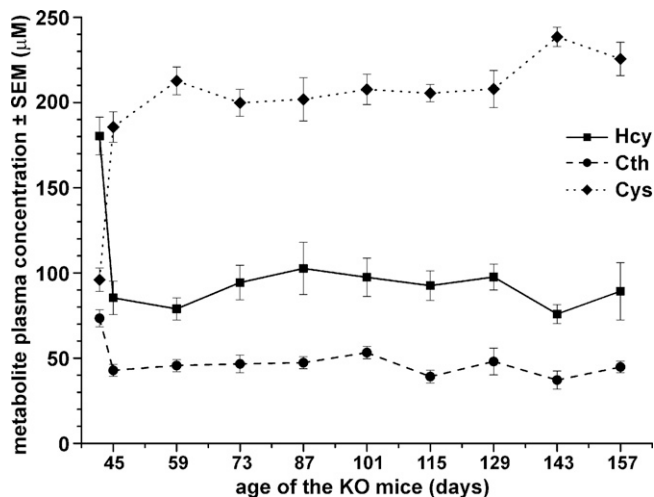
Figure 6. Long-term treatment of the KO mice with 20NHS PEG-CBS sustains an improved plasma metabolite profile. The KO mice (n = 5 M + 7 F) were treated 3 times a week with 20NHS PEG-CBS (SC, 7.5 mg/kg) from d 2 of age for ~5 mo. The initial levels at d 42 do not represent true basal concentrations of the metabolites prior to the treatment initiation because KO mice were treated from birth to prevent neonatal lethality. Instead, the initial levels correspond to plasma concentration of the metabolites 72 h after the injection (*i.e.*, after a weekend washout), when mice were old enough to survive blood collection. Relevant sulfur amino acids are shown: Hcy (solid line with squares), Cth (dashed line with circles), and Cys (dotted line with diamonds). Symbols represent an average value from individual mice. Error bars indicate SEM.

treated mice can be associated with diet as well as with incomplete metabolic control of Hcy levels. In studies described herein, the KO mice were maintained on a standard rodent chow without Met restriction. Such constant flux of Met most likely resulted in increased production of

Hcy (Supplemental Table 1) and reversed the synthesis of SAH by SAH hydrolase. This hypothesis is supported by the observation that SAM levels of the treated mice were similar to or lower than levels in the control mice. The long-term consequences of slightly elevated SAH and normal or low-normal SAM in tissues are unknown and warrant further studies. Because Cys available for GSH synthesis was found substantially decreased in the liver of KO mice, we anticipated that GSH levels would be impaired, as shown previously (8, 16). However, we did not observe any significant differences in GSH levels in plasma and either tissue among age-matched WT, KO, and PEG-CBS–treated KO mice. We believe that tissue metabolites from 2-wk-old untreated KO mice were incorrectly compared with 7- to 20-wk-old WT control mice (16) because the levels of GSH may differ with age of mice, and, more importantly, the previously observed liver GSH levels of infant KO mice are in line with our findings (8). Intracellular levels of GSH are critical for the cellular defense and redox signaling and thus are heavily regulated (17). Therefore, it seems plausible that, even under severe HCU, GSH synthesis is prioritized as essential and kept unaffected, particularly during the neonatal period.

Previous microscopic evaluation of liver sections from KO mice showed severe steatosis with hepatocellular necrosis (5, 6, 8, 18). These observations were confirmed in this study in the untreated KO mice. However, as evident from both light (Fig. 4) and electron (Fig. 5) microscopy, treatment of KO mice from 2 d of age, particularly with 20NHS PEG-CBS, prevented liver disease. The etiology of liver disease in HCU is still unclear, with oxidative damage likely playing a central role (18). Liver disease in patients with HCU is generally silent; hepatic function test results are usually normal, and biopsies are rare nowadays (19).

Figure 7. Bone mineralization and body composition of the KO mice at 5 mo of age. Because the KO mouse phenotype is neonatally lethal, all mice were treated with 3 weekly injections of 20NHS PEG-CBS (SC, 7.5 mg/kg) from d 2 of age to allow their survival into adulthood. At 35 d of age, the mice were randomized into 3 groups: healthy control mice consisting of heterozygous KO mice (n = 4 M + 6 F; black bars); affected KO mice (n = 5 M + 13 F; white bars), which were left untreated from d 35 on; and treated KO mice (n = 5 M + 7 F; hatched bars) continued receiving treatment as during the initial 5 wk. The DXA scans were performed when the mice reached ~5 mo of age. Individual panels show bone mineral density (*A*), bone mineral content (*B*), total mass (*C*), lean mass (*D*), and fat content (*E*). Bars represent an average value from individual mice. Error bars indicate SEM. *$P < 0.05$, **$P < 0.01$, ***$P < 0.001$.
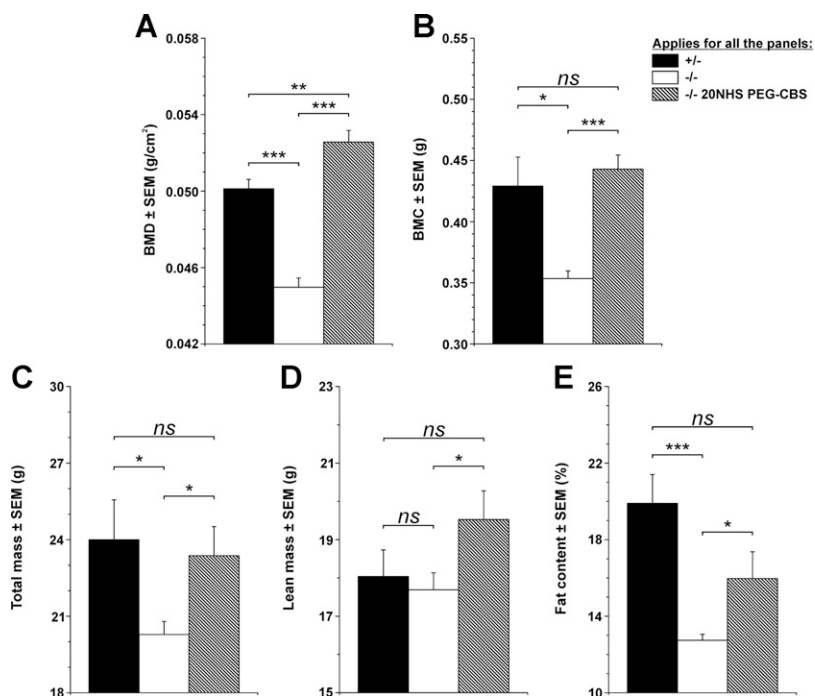
However, past microscopic analyses showed that patients with HCU exhibit similar findings as KO mice, namely steatosis, abnormal mitochondria, and depleted cellular glycogen (19–21). Furthermore, no effect of pyridoxine supplementation on the ultrastructure of hepatocytes was found despite improved plasma metabolites (20).

Skeletal and connective tissue abnormalities, particularly lens dislocation, marfanoid features with a thin and tall stature, and osteoporosis, represent the most common phenotypical features, particularly in patients with HCU with the severe pyridoxine nonresponsive form of the disease (1, 22). In this study, we showed that KO mice are a good model of the human osteoporosis phenotype. Early treatment with 20NHS PEG-CBS prevented the loss of bone mineralization and fat content in KO mice. Although early diagnosis and lifelong treatment with good biochemical control can prevent osteoporosis in patients with HCU, loss of biochemical control due to common noncompliance with the treatment can be associated with progression of skeletal complications (4, 23). Unlike the case of liver disease, efficacy of enzyme replacement on osteoporosis and body composition in patients with HCU can be monitored longitudinally using a noninvasive technique, such as DXA. Thus, our results indicate that assessment of osteoporosis and/or body composition in clinical trials may represent a suitable clinically relevant endpoint in addition to the biochemical markers.

Serious long-term complications, such as thromboembolic events, seem to be prevented when plasma total Hcy is maintained as low as possible, ideally below 100 μM (4, 24). For patients with HCU struggling with the protein-restricted diet, it is not an attainable goal. Here we were able to achieve this aim with ERT alone in the most severely affected CBS-KO mice without any dietary restriction or supplementation. It is unclear how the 20NHS PEG-CBS will be tolerated immunologically and whether the overproduction of Cth observed in this study will have any clinical consequences (7), although inherited cystathioninuria is considered a benign condition (25). However, our nonclinical data also argue that the earlier the treatment is initiated, the less damage is caused, and complete prevention of clinical symptoms is feasible. This is an important aspect because it relies on early diagnosis currently mediated only *via* newborn screening or family history (4, 26) and treatment since the neonatal period.

In summary, the administration of PEG-CBS to CBS-KO mice reversed the lethal phenotype. The ERT prevented liver disease in the treated KO mice, with histologic and electron microscopic observations indistinguishable from healthy heterozygous control mice. The continuous administration of ERT sustained an improved plasma metabolic profile, which has been mirrored in tissues and resulted in the prevention of osteoporosis, a characteristic symptom of HCU. FJ

ACKNOWLEDGMENTS

AUTHOR CONTRIBUTIONS

T. Majtan designed and performed animal studies, prepared and analyzed PEG-CBS conjugates, analyzed data, prepared figures, wrote the initial draft, and coordinated the collaboration; H. Hůlková performed liver histology and interpreted the findings; I. Park took care of the animal colony and performed the animal studies; J. Krijt determined sulfur amino acid metabolites in tissues and matching plasmas; V. Kožich coordinated liver histology and tissue metabolite analyses; E. M. Bublil coordinated the collaboration and analyses; J. P. Kraus conceived and designed the studies, reviewed the data, and coordinated the project; and all authors reviewed the draft, contributed to its revisions, and approved the final manuscript.

REFERENCES

1. Mudd, S. H., Levy, H. L., and Kraus, J. P. (2001) Disorders of transsulfuration. In *The Metabolic and Molecular Bases of Inherited Disease* (Scriver, C. R., Beaudet, A. L., Sly, W. S., Valle, D., Childs, B., Kinzler, K., and Vogelstein, B., eds), pp. 2007–2056, McGraw-Hill, New York

2. Moorthie, S., Cameron, L., Sagoo, G. S., Bonham, J. R., and Burton, H. (2014) Systematic review and meta-analysis to estimate the birth prevalence of five inherited metabolic diseases. *J. Inherit. Metab. Dis.* **37**, 889–898

3. Majtan, T., Pey, A. L., Ereño-Orbea, J., Martínez-Cruz, L. A., and Kraus, J. P. (2016) Targeting cystathionine beta-synthase misfolding in homocystinuria by small ligands: state of the art and future directions. *Curr. Drug Targets* **17**, 1455–1470

4. Morris, A. A., Kožich, V., Santra, S., Andria, G., Ben-Omran, T. I., Chakrapani, A. B., Crushell, E., Henderson, M. J., Hochuli, M., Huemer, M., Janssen, M. C., Maillot, F., Mayne, P. D., McNulty, J., Morrison, T. M., Ogier, H., O'Sullivan, S., Pavlíková, M., de Almeida, I. T., Terry, A., Yap, S., Blom, H. J., and Chapman, K. A. (2017) Guidelines for the diagnosis and management of cystathionine beta-synthase deficiency. *J. Inherit. Metab. Dis.* **40**, 49–74

5. Bublil, E. M., Majtan, T., Park, I., Carrillo, R. S., Hůlková, H., Krijt, J., Kožich, V., and Kraus, J. P. (2016) Enzyme replacement with PEGylated cystathionine β-synthase ameliorates homocystinuria in murine model. *J. Clin. Invest.* **126**, 2372–2384

6. Watanabe, M., Osada, J., Aratani, Y., Kluckman, K., Reddick, R., Malinow, M. R., and Maeda, N. (1995) Mice deficient in cystathionine β-synthase: animal models for mild and severe homocyst(e)inemia. *Proc. Natl. Acad. Sci. USA* **92**, 1585–1589

7. Majtan, T., Park, I., Carrillo, R. S., Bublil, E. M., and Kraus, J. P. (2017) Engineering and characterization of an enzyme replacement therapy for classical homocystinuria. *Biomacromolecules* **18**, 1747–1761

8. Maclean, K. N., Sikora, J., Kožich, V., Jiang, H., Greiner, L. S., Kraus, E., Krijt, J., Crnic, L. S., Allen, R. H., Stabler, S. P., Elleder, M., and Kraus, J. P. (2010) Cystathionine beta-synthase null homocystinuric mice fail to exhibit altered hemostasis or lowering of plasma homocysteine in response to betaine treatment. *Mol. Genet. Metab.* **101**, 163–171

9. Allen, R. H., Stabler, S. P., and Lindenbaum, J. (1993) Serum betaine, *N,N*-dimethylglycine and *N*-methylglycine levels in patients with cobalamin and folate deficiency and related inborn errors of metabolism. *Metabolism* **42**, 1448–1460

10. Krijt, J., Dutá, A., and Kozich, V. (2009) Determination of S-adenosylmethionine and S-adenosylhomocysteine by LC-MS/MS and evaluation of their stability in mice tissues. *J. Chromatogr. B Analyt. Technol. Biomed. Life Sci.* **877**, 2061–2066

11. Kožich, V., Krijt, J., Sokolová, J., Melenovská, P., Ješina, P., Vozdek, R., Majtán, T., and Kraus, J. P. (2016) Thioethers as markers of hydrogen sulfide production in homocystinurias. *Biochimie* **126**, 14–20

12. Komrower, G. M., Lambert, A. M., Cusworth, D. C., and Westall, R. G. (1966) Dietary treatment of homocystinuria. *Arch. Dis. Child.* **41**, 666–671

13. Barber, G. W., and Spaeth, G. L. (1967) Pyridoxine therapy in homocystinuria. *Lancet* **1**, 337

14. Smolin, L. A., Benevenga, N. J., and Berlow, S. (1981) The use of betaine for the treatment of homocystinuria. *J. Pediatr.* **99**, 467–472

15. Walter, J. H., Wraith, J. E., White, F. J., Bridge, C., and Till, J. (1998) Strategies for the treatment of cystathionine β-synthase deficiency: the experience of the Willink Biochemical Genetics Unit over the past 30 years. *Eur. J. Pediatr.* **157** (Suppl 2), S71–S76

16. Vitvitsky, V., Dayal, S., Stabler, S., Zhou, Y., Wang, H., Lentz, S. R., and Banerjee, R. (2004) Perturbations in homocysteine-linked redox homeostasis in a murine model for hyperhomocysteinemia. *Am. J. Physiol. Regul. Integr. Comp. Physiol.* **287**, R39–R46

17. Dickinson, D. A., and Forman, H. J. (2002) Glutathione in defense and signaling: lessons from a small thiol. *Ann. N. Y. Acad. Sci.* **973**, 488–504

18. Robert, K., Nehmé, J., Bourdon, E., Pivert, G., Friguet, B., Delcayre, C., Delabar, J. M., and Janel, N. (2005) Cystathionine beta synthase deficiency promotes oxidative stress, fibrosis, and steatosis in mice liver. *Gastroenterology* **128**, 1405–1415

19. Mack, C. L., Emerick, K. M., Kovarik, P., and Charrow, J. (2001) Early speech delay and hepatitis as presenting signs of homocystinuria. *J. Pediatr. Gastroenterol. Nutr.* **33**, 221–223

20. Gaull, G. E., and Schaffner, F. (1971) Electron microscopic changes in hepatocytes of patients with homocystinuria. *Pediatr. Res.* **5**, 23–32

21. Gaull, G., Sturman, J. A., and Schaffner, F. (1974) Homocystinuria due to cystathionine synthase deficiency: enzymatic and ultrastructural studies. *J. Pediatr.* **84**, 381–390

22. Schedewie, H., Willich, E., Gröbe, H., Schmidt, H., and Müller, K. M. (1973) Skeletal findings in homocystinuria: a collaborative study. *Pediatr. Radiol.* **1**, 12–23

23. Parrot, F., Redonnet-Vernhet, I., Lacombe, D., and Gin, H. (2000) Osteoporosis in late-diagnosed adult homocystinuric patients. *J. Inherit. Metab. Dis.* **23**, 338–340

24. Wilcken, D. E. L., and Wilcken, B. (1997) The natural history of vascular disease in homocystinuria and the effects of treatment. *J. Inherit. Metab. Dis.* **20**, 295–300

25. Kraus, J. P., Hasek, J., Kozich, V., Collard, R., Venezia, S., Janosíková, B., Wang, J., Stabler, S. P., Allen, R. H., Jakobs, C., Finn, C. T., Chien, Y. H., Hwu, W. L., Hegele, R. A., and Mudd, S. H. (2009) Cystathionine gamma-lyase: clinical, metabolic, genetic, and structural studies. *Mol. Genet. Metab.* **97**, 250–259

26. Huemer, M., Kožich, V., Rinaldo, P., Baumgartner, M. R., Merinero, B., Pasquini, E., Ribes, A., and Blom, H. J. (2015) Newborn screening for homocystinurias and methylation disorders: systematic review and proposed guidelines. *J. Inherit. Metab. Dis.* **38**, 1007–1019

Supplementary Table 1. Plasma and tissue levels of sulfur metabolites in untreated or 20NHS PEG-CBS-injected KO mice compared to healthy untreated +/+ mice. Total homocysteine and cysteine were determined in plasma, while nonprotein-bound fractions of these thiols were measured in tissue homogenates. Treated KO mice were dosed 3x a week 7.5 mg/kg from day 2 of age. Each group consisted of three to four 18 days old mice. Data expressed as averages ± standard error of the means were compared using multivariate ANOVA followed by Tukey's post hoc test to determine significance: * $p<0.05$, ** $p<0.01$, *** $p<0.001$, *ns* – non-significant. Significance values in parentheses refer to comparisons of the respective group (either +/+ WT or -/- KO) to the 20NHS PEG-CBS-treated -/- mice.

		+/+ (WT) (n = 3)	-/- (KO) (n = 4)	-/- 20NHS PEG-CBS (n = 3)
Hcy	Plasma (µM)	10.1±0.7 (*)	261.4±12.9 (***)	52.8±6.8
	Liver (nmols/g)	9.2±0.4 (*ns*)	63.4±8.6 (*)	22.4±3.4
	Kidney (nmols/g)	4.0±1.5 (*ns*)	23.7±2.7 (*)	2.3±0.0
	Brain (nmols/g)	4.0±0.9 (*ns*)	24.8±7.8 (*)	1.1±0.1
Cys	Plasma (µM)	237.9±9.2 (*ns*)	95.9±8.1 (***)	211.7±11.5
	Liver (nmols/g)	257.8±13.7 (*ns*)	110.6±13.0 (*)	205.2±27.4
	Kidney (nmols/g)	239.8±15.5 (*ns*)	239.8±34.5 (*ns*)	282.8±17.5
	Brain (nmols/g)	55.0±3.6 (*ns*)	51.4±1.4 (*ns*)	56.8±3.0
Cth	Plasma (µM)	2.8±0.1 (**)	0.06±0.02 (**)	133.2±9.1
	Liver (nmols/g)	24.9±7.8 (*ns*)	0.48±0.11 (**)	18.9±1.8
	Kidney (nmols/g)	6.7±1.0 (***)	0.47±0.06 (**)	178.5±0.9
	Brain (nmols/g)	69.0±18.9 (*)	1.29±0.27 (*)	8.5±1.1
Met	Plasma (µM)	87.7±6.0 (*ns*)	483.7±51.7 (*)	99.2±5.4
	Liver (nmols/g)	39.2±2.1 (*ns*)	511.0±66.8 (*)	25.5±3.4
	Kidney (nmols/g)	61.2±13.2 (*ns*)	466.2±112.8 (*)	53.3±2.9
	Brain (nmols/g)	61.6±3.4 (*ns*)	616.0±71.2 (*)	68.6±4.2
GSH	Plasma (µM)	34.7±2.4 (*ns*)	31.3±0.6 (*ns*)	27.7±1.5
	Liver (nmols/g)	4479±61 (*ns*)	4376±317 (*ns*)	4547±215
	Kidney (nmols/g)	1021±414 (*ns*)	1894±119 (*)	1392±24
	Brain (nmols/g)	1494±76 (*ns*)	1518±49 (*ns*)	1460±7
SAM	Plasma (nM)	350±5 (*ns*)	800±70 (**)	282±23
	Liver (nmols/g)	28.5±4.2 (*ns*)	577±35 (***)	24.4±5.5
	Kidney (nmols/g)	22.1±1.2 (*ns*)	30.2±1.7 (*)	23.2±1.5
	Brain (nmols/g)	28.6±2.5 (*ns*)	29.8±5.6 (*ns*)	21.5±0.7
SAH	Plasma (nM)	56±2 (**)	6560±1080 (**)	91±4
	Liver (nmols/g)	36.4±1.4 (*)	631±88 (*)	85.8±10.8
	Kidney (nmols/g)	2.2±0.2 (*)	71.4±9.9 (**)	9.8±1.9
	Brain (nmols/g)	5.7±0.8 (*)	82.2±13.3 (**)	14.0±1.4
SAM/SAH	Plasma	6.1±0.4 (***)	0.12±0.01 (*)	3.1±0.4
	Liver	0.8±0.1 (*)	0.94±0.09 (**)	0.28±0.03
	Kidney	10.3±1.2 (*)	0.44±0.07 (*)	2.5±0.4
	Brain	5.1±0.3 (**)	0.36±0.01 (**)	1.6±0.1